# Short Papers

## On the Location of Leaky Wave Poles for a Grounded Dielectric Slab

Chung-I G. Hsu, Roger F. Harrington, Joseph R. Mautz, and Tapan K. Sarkar

*Abstract*—**A simple numerical procedure is implemented to find the loci of the TE and TM leaky wave poles for a grounded dielectric slab as the frequency or the thickness varies. Information on how these complex poles are distributed is very important when various deformed integration paths for Sommerfeld integrals are considered.**

### I. Introduction

It is well known that the electromagnetic fields arising from a dipole in a layered medium in an open region can be expressed in terms of an improper integral [1] to account for the continuous spectra. In order to perform this integration accurately and efficiently, the integration path must be deformed off the real axis in some cases. Various deformed paths have been considered by many researchers, e.g., Newman and Forrai [2], Michalski and Zheng [3], Fang and Chew [4], and Sarkar [5], to name but a few. For half-space problems, there are only two surface wave poles located on either sheets I and IV or sheets II and III of the Riemann surface [3], [6], depending on the constitutive parameters of the two media. For a grounded dielectric slab, besides a finite number of surface wave poles, there are an infinite number of leaky wave poles [7]–[9]. If the branch cut is properly chosen [3], [7], [9], then all the surface wave poles are located on the top sheet (proper sheet, or sheet I), whereas all the leaky wave poles are located on the bottom sheet (improper sheet, or sheet II) of the Riemann surface. The locations of the leaky wave poles are immaterial if the integration path stays on sheet I. In order to improve the computational efficiency, deforming the path to sheet II is desirable in some cases, e.g., the steepest descent method of integration for far fields, where part of the path enters sheet II [9], [10], [13]. In this case, precise information on how these leaky wave poles are distributed is very important unless the residues of these leaky wave poles are negligible. Some researchers [10], [11], when applying the steepest descent method of integration or its approximate version, the so-called saddle point method, only take into account surface wave poles. It is clear from the next section that their results are correct if the dielectric slab is thin and if the observation point is not too close to the interface. However, when the thickness of the slab is moderate or when the observation point is close to the interface, some of the leaky wave poles, not too far away from the saddle point, may have been captured.

Manuscript received April 30, 1990; revised August 15, 1990. This work was supported by the Office of Naval Research, Arlington, VA 22217, under Contract N00014-88-K-0027 and by the U.S. Army Research Office, Research Triangle Park, NC 27709, under Contract DAAL03-88-K-0133.

The authors are with the Department of Electrical and Computer Engineering, Syracuse University, Syracuse, NY 13244-1240.

IEEE Log Number 9041075.

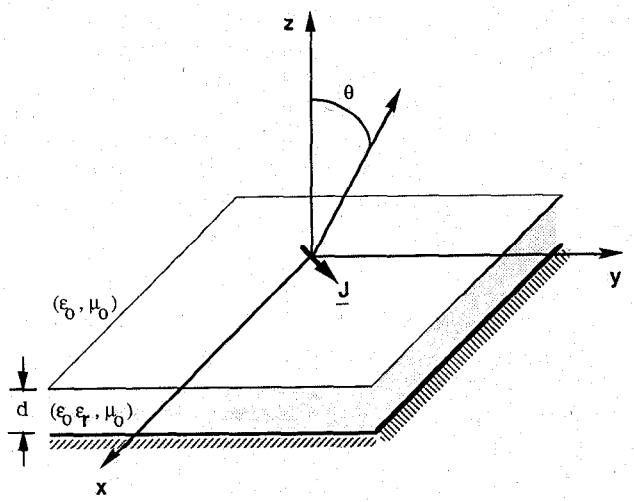


Fig. 1. The grounded dielectric slab.

The locations of the TE or TM leaky wave poles can be found by solving for the roots of two simultaneous transcendental equations [7], [9], which are then mapped to the complex plane of the integration variable. Although standard root searching routines could be applied, we gain no idea how these roots are distributed in the complex plane, since there are an infinite number of them for a given frequency. It is the purpose of this short communication to give a simple numerical procedure for finding the loci of the leaky wave poles as the frequency or the thickness varies. Thus, this gives us the desired information.

### II. Root Loci

The geometry of the grounded dielectric slab is shown in Fig. 1. For simplicity, we assume that the slab is nonmagnetic and lossless. The constitutive parameters for the half space and the slab are $(\epsilon_0, \mu_0)$ and $(\epsilon_0\epsilon_r, \mu_0)$, respectively. The thickness of the slab is $d$. The locations of the surface and leaky wave poles are the roots of [9], [10], [12]

$$D_{\mathrm{TE}} = j\sqrt{1-\xi^2} + \sqrt{\epsilon_r - \xi^2}\cot\left(\sqrt{\epsilon_r - \xi^2}\,k_0 d\right) \qquad (1)$$

for the TE case and

$$D_{\mathrm{TM}} = j\epsilon_r\sqrt{1-\xi^2} - \sqrt{\epsilon_r - \xi^2}\tan\left(\sqrt{\epsilon_r - \xi^2}\,k_0 d\right) \qquad (2)$$

for the TM case. Here, $\xi$ is the normalized parameter such that $k_\rho = \xi k_0$ is the transverse wavenumber or integration variable for the Sommerfeld integral in terms of a transmission line representation in the $z$ direction [9], [10], where $z$ is perpendicular to the interface. For convenience, the branch cut is chosen to be the line such that $\mathrm{Im}\{\sqrt{1-\xi^2}\} = 0$ [3], [9], [10], [13], as shown in Fig. 2. When this branch cut is chosen, the roots of (1) and (2) on sheets I and II of the complex $\xi$ plane are the surface wave and leaky wave poles, respectively. It is well known that the surface wave poles are real and confined to the region

0018-9480/91/0200-0346$01.00 ©1991 IEEE

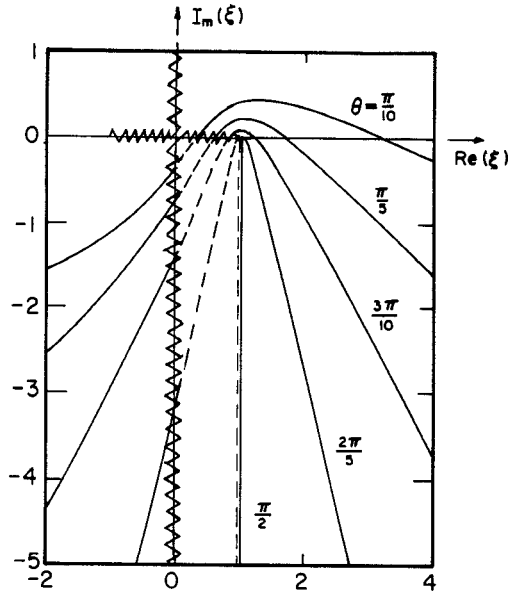


Fig. 2. Steepest descent paths in the complex $\xi$ plane for different observation angles, where the solid line is on the top sheet, the dotted line is on the bottom sheet, and the zigzag line is the branch cut.

$1 < \xi < \sqrt{\epsilon_r}$, and there are a finite number of them [10], [12]. Furthermore, it can be shown that the leaky wave poles assume both real and complex values, and there are an infinite number of them [7], [9]. Note that in [14], the wave corresponding to the leaky wave pole of purely real value is specifically termed open mode. It is understood that the magnitude of the leaky mode increases with $z$. A source within the slab must excite many leaky modes, which in turn interfere destructively to ultimately generate decreased response as $z$ increases [14]. A simple graphical procedure [9], [12] can be employed to find the real roots of (1) and (2), as shown in Fig. 3(a) and (b), respectively. In these two figures,

$$X = k_0 d\sqrt{\epsilon_r - \xi^2} \quad \text{and} \quad B = k_0 d\sqrt{\epsilon_r - 1}\,. \tag{3}$$

The intersecting points on the upper and the lower parts are related to the surface and leaky wave poles on the real $\xi$ axis, respectively. Although there are infinitely many branches of curves for a tangent or cotangent function, only six of them are plotted here.

There is only one pole associated with curve *1* in Fig. 3(a). It is a surface wave pole if $B > \pi/2$ and a leaky wave pole in the regions $1 < \xi < \sqrt{\epsilon_r}$ or $\sqrt{\epsilon_r} < \xi < \infty$ if $1 < B < \pi/2$ or $0 < B < 1$, respectively [7], [9]. Likewise, the pole associated with curve *1* in Fig. 3(b) is always a surface wave pole. Clearly, there are two poles associated with the rest of the curves in both figures. As an illustration, let curve *2* in Fig. 3(a) be examined. If $B > 3\pi/2$, the semicircle intersects with curve *2* at two points, one corresponding to the surface wave pole and the other to the leaky wave pole, both of which have real values between 1 and $\sqrt{\epsilon_r}$ in the complex $\xi$ plane. As $B$ decreases and becomes smaller than $3\pi/2$, the surface wave pole in the $\xi$ plane falls down to sheet II from sheet I at $\xi = 1$, which is the branch point. Then it becomes a leaky wave pole and moves to the right, whereas the original leaky wave pole stays on the same sheet and moves to the left. As $B$ reaches a value $B_0$, such that in Fig. 3(a) the semicircle is tangent to curve *2*, these two leaky wave poles in the $\xi$ plane merge into one. If we reduce $B$ further, then in Fig. 3(a) the semicircle does not intersect with curve *2* any more, and in the $\xi$ plane the poles move symmetrically off the real axis on sheet II. It is understood that the poles in the $\xi$ plane move

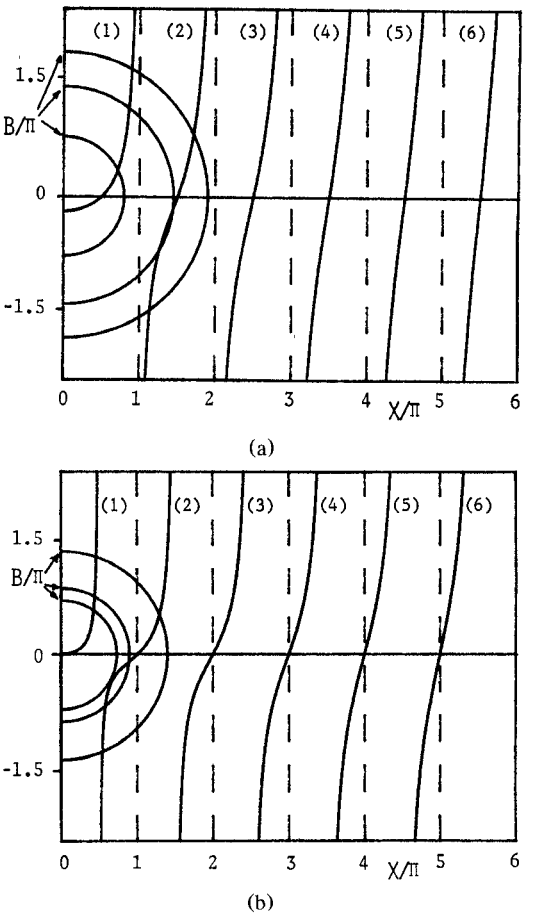


Fig. 3. Graphic solution for the TE and TM surface and leaky wave modes, where the semicircles represent $\pm\sqrt{B^2 - X^2}$. (a) TE: $(B^2 - X^2)^{1/2} = -X\cot X$. (b) TM: $(B^2 - X^2)^{1/2} = X/\epsilon_r \tan X$.

smoothly as $B$ varies. Based on the above observation, the numerical procedure for finding the locus of the leaky wave poles in the $\xi$ plane associated with each curve in Fig. 3(a) and (b) is as follows.

1) Find $B_0$ and the corresponding $\xi$, called $\xi_0$. Since $\xi_0$ is real, this step is straightforward.
2) Search for a new root $\xi_1$ for the parameter $B_1 = B_0 - \Delta B$ with $\xi_0 - j\delta$ as the initial searching point, where both $\Delta B$ and $\delta$ are small positive numbers.
3) Search for new roots $\xi_{n+1}$ for the parameters $B_{n+1} = B_n - \Delta B_n$, $n = 1, 2, 3, \cdots$, with $\xi_n$ as the initial searching points.

If the $\Delta B_n$'s are reasonably small, a few iterations of steps 2 and 3 give satisfactory results using a Newton–Raphson algorithm. The same procedure can be repeated to generate the locus associated with each curve in Fig. 3(a) and (b). Since when $\xi$ is a root of (1) or (2), then $-\xi$ and $\pm\xi^*$ are also roots, we show only the loci in the fourth quadrant (these being the leaky wave poles that matter for a time dependence $e^{j\omega t}$). Figs. 4 to 7 show the loci of the leaky wave poles for $\epsilon_r = 4$ and 9, respectively. From the magnified versions of these figures, it is qualitatively true that each locus goes into the fourth quadrant with the right angle, which is not shown here. Furthermore, careful scrutiny of these figures reveals that the TM poles approach the real axis faster than do the TE poles as $B$ increases from zero. Furthermore, for both the TE and TM cases, the poles associated with the first two or three curves shown in Fig. 3(a) and (b) approach the real axis faster than those associated with the higher num-

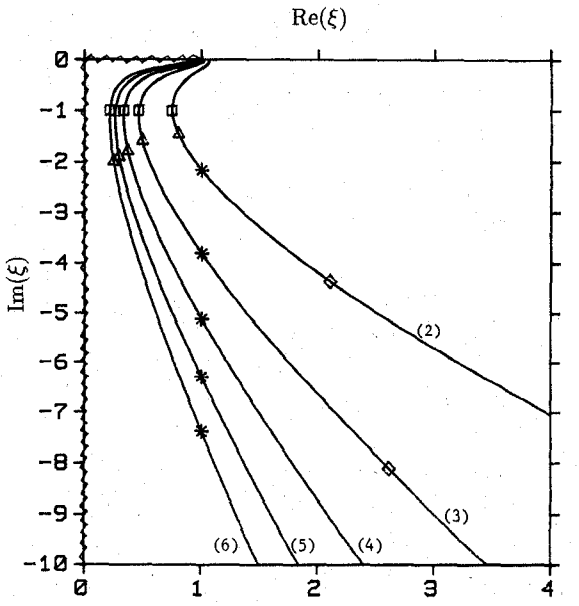


| B/π | (2) | (3) | (4) | (5) | (6) |
|---|---|---|---|---|---|
| □ | 1.1484 | 1.9309 | 2.7060 | 3.4798 | 4.2553 |
| △ | 1.0202 | 1.6768 | 2.2394 | 2.8111 | 3.3562 |
| * | 0.8425 | 0.9794 | 1.0848 | 1.1671 | 1.2354 |
| ◇ | 0.5003 | 0.4990 | — | — | — |

Fig. 4. Loci of the TE leaky wave poles in the complex $\xi$ plane, $\epsilon_r = 4$.

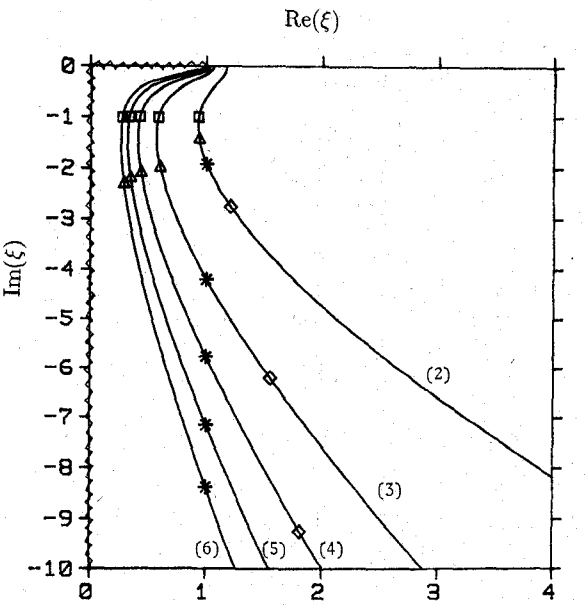


| B/π | (2) | (3) | (4) | (5) | (6) |
|---|---|---|---|---|---|
| □ | 1.3261 | 2.2285 | 3.1282 | 4.0230 | 4.9142 |
| △ | 1.2473 | 1.9433 | 2.6882 | 3.4058 | 4.9075 |
| * | 1.1576 | 1.3421 | 1.5031 | 1.6272 | 1.7365 |
| ◇ | 1.0000 | 1.0011 | 1.0021 | — | — |

Fig. 6. Loci of the TE leaky wave poles in the complex $\xi$ plane, $\epsilon_r = 9$.

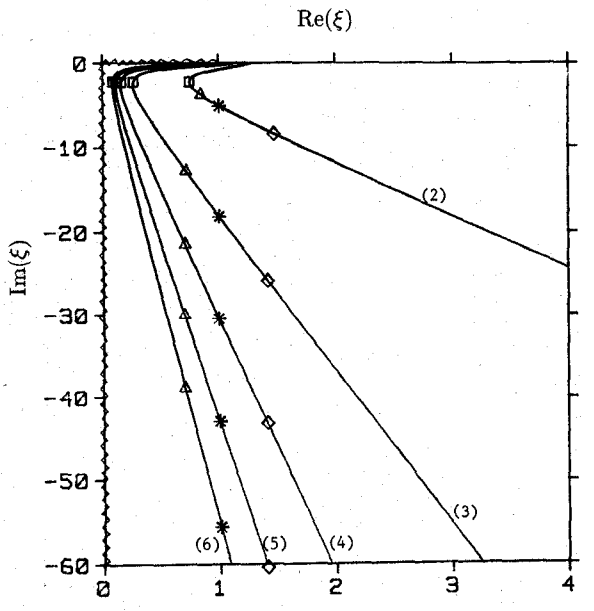


| B/π | (2) | (3) | (4) | (5) | (6) |
|---|---|---|---|---|---|
| □ | 0.2954 | 0.8623 | 1.4343 | 2.0072 | 2.5856 |
| △ | 0.2013 | 0.2003 | 0.2004 | 0.2011 | 0.2002 |
| * | 0.1578 | 0.1421 | 0.1417 | 0.1409 | 0.1400 |
| ◇ | 0.1001 | 0.1001 | 0.1001 | 0.1004 | — |

Fig. 5. Loci of the TM leaky wave poles in the complex $\xi$ plane, $\epsilon_r = 4$.

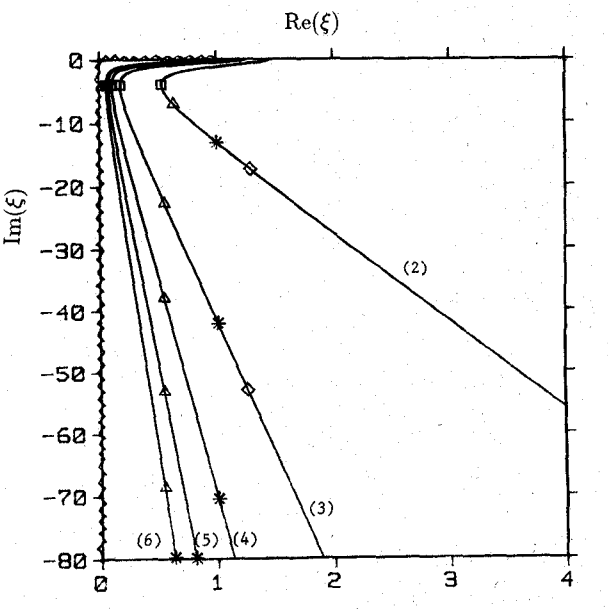


| B/π | (2) | (3) | (4) | (5) | (6) |
|---|---|---|---|---|---|
| □ | 0.2860 | 0.8547 | 1.4239 | 1.9939 | 2.5609 |
| △ | 0.1856 | 0.1851 | 0.1855 | 0.1859 | 0.1853 |
| * | 0.1053 | 0.1006 | 0.1003 | 0.1240 | 0.1596 |
| ◇ | 0.0801 | 0.0801 | — | — | — |

Fig. 7. Loci of the TM leaky wave poles in the complex $\xi$ plane, $\epsilon_r = 9$.

bered curves. This explains why only the lower ordered leaky poles are important for a thin slab when the steepest descent path is adopted. A comparison of Fig. 2, which shows the steepest descent paths for various observation angles, with Figs. 4 to 7 demonstrates that many leaky wave poles can be captured by the deformation, depending on the observation angle and physical parameters of the slab. The residues of the leaky wave poles are highly attenuated in the far field, as claimed by Fang and Chow [4]. In fact, they completely ignored the residues of the leaky poles for separation distance $k_0 r > 2\pi$ and observation angle $\theta = \pi/2$, i.e., on the interface. However, it is clear from [15] that for some values of the dielectric constant and height, the closeness of the leaky wave poles to the steepest descent path must still be taken into account, even for $k_0 r = 100$ and $0 < \theta < \pi/2$. Although the physical parameters employed in [4] and [15] are different, our purpose is to emphasize that care must be taken when ignoring the residues of the leaky wave poles. Moreover, without knowing the locations or the loci of the leaky wave poles, this cannot be done satisfactorily.

## III. Concluding Remarks

A simple numerical procedure for finding the loci of TE and TM leaky wave poles as the frequency or the thickness of the slab varies is presented. These loci provide important information when the integration path of the Sommerfeld integral for the grounded dielectric slab problem is deformed into the "improper" sheet of the Riemann surface. The accuracy of the loci has been checked extensively against contour plots of expressions (1) and (2) with the $B$'s as parameters.

## Acknowledgment

The authors would like to thank Dr. D. Zheng at Texas A&M University for valuable discussions.

## References

[1] L. B. Felsen and N. Marcuvitz, *Radiation and Scattering of Waves*. Englewood Cliffs, NJ: Prentice Hall, 1973.
[2] E. H. Newman and D. Forrai, "Scattering from a microstrip patch," *IEEE Trans. Antennas Propagat.*, vol. AP-35, pp. 245–251, Mar. 1987.
[3] K. Michalski and D. Zheng, "Modeling antennas and scatterers of arbitrary shape embedded in layered dielectric media," Tech. Rep., Dept. Elec. Eng., Texas A&M University, Nov. 1989.
[4] D. G. Fang and Y. L. Chow, "The Green's function along the microstrip substrate from a horizontal magnetic dipole," *J. Appl. Phys.*, vol. 54, pp. 33–38, Jan. 1983.
[5] T. K. Sarkar, "Analysis of arbitrarily oriented thin wire antennas over a plane imperfect ground," *Arc. Elek. Übertragung.*, vol. 31, pp. 449–457, 1977.
[6] A. Banõs, *Dipole Radiation in the Presence of a Conducting Half-Space*. New York: Pergamon Press, 1966.
[7] S. Barkeshli, "Efficient approaches for evaluating the planar microstrip Green's function and its applications to the analysis of microstrip antennas," Ph.D. dissertation, Dept. Elec. Eng., Ohio State Univ., 1988.
[8] M. Marin, S. Barkeshli, and P. H. Pathak, "On the location of proper and improper surface wave poles for the grounded dielectric slab," *IEEE Trans. Antennas Propagat.*, vol. 38, pp. 570–573, Apr. 1990.
[9] R. E. Collin, *Field Theory of Guided Waves*. New York: McGraw-Hill, 1960.
[10] J. R. Mosig and F. E. Gardiol, "A dynamical radiation model for microstrip structures," in *Advances in Electronics and Electron Physics*, vol. 59. New York: Academic Press, 1982, pp. 139–237.
[11] G. N. Tsandoulas, "Excitation of a grounded dielectric slab by a horizontal dipole," *IEEE Trans. Antennas Propagat.*, vol. AP-17, pp. 156–161, Mar. 1969.
[12] R. F. Harrington, *Time-Harmonic Electromagnetic Fields*. New York: McGraw-Hill, 1961.
[13] T. Tamir and A. A. Oliner, "Guided complex waves: Part 1," *Proc. Inst. Elec. Eng.*, vol. 110, pp. 310–324, Feb. 1963.
[14] K. G. Budden, *The Wave-Guide Mode Theory of Wave Propagation*. Englewood Cliffs, NJ: Prentice-Hall, 1961.
[15] G. D. Bernard and A. Ishimaru, "On complex waves," *Proc. Inst. Elec. Eng.*, vol. 114, pp. 43–49, Jan. 1967.

# Dispersion Characteristics of Strip Dielectric Waveguides

Kin S. Chiang

***Abstract*—A simple and accurate dispersion relation is derived for the guided modes of a strip dielectric waveguide. This relation shows explicitly the effect of the width of the waveguide and involves only the solution for a single three-layer slab waveguide. It is discovered that there always exists a strip waveguide with a specific aspect ratio in which the $E^x_{mn}$ and $E^y_{mn}$ modes propagate at the same phase velocity.**

## I. Introduction

A strip dielectric waveguide of the type shown in Fig. 1(a) is a basic and important wave-guiding structure and serves as a building block in many transmission devices at millimeter-wave and optical frequencies [1]–[4]. While exact analytical solutions are not available, this waveguide has been analyzed by various semianalytical and numerical methods, which include the effective-index method [1], [2], [5], [6], Marcatili's method [7], the mode-matching method [8], the finite-element method [9], [10], the finite-difference method [11], [12], and the weighted-index method [13]. However, many of these methods [8]–[13] require massive computation and the physical properties of the waveguide are not apparent in such analyses.

In this paper a simple approximate expression is derived to describe explicitly the dispersion characteristics of the guided modes of a strip waveguide. The accuracy of this expression is confirmed by comparison with results from other methods. The use of this expression should significantly simplify the study and design of strip waveguides.

## II. Analysis and Results

We consider the embossed wave-guiding structure as shown in Fig. 1(a), which is commonly referred to as a strip waveguide, an insulated image guide, or a special type of rib waveguide. We adopt here the optics terminology by denoting $n_1$, $n_2$, and $n_3$ ($n_1 > n_2 > n_3$) as the refractive indexes of the strip, the substrate, and the superstrate (usually air), respectively. The strip has a height $2b$ and a width $2a$ and the substrate and the superstrate are assumed unbounded. The guided mode of such a waveguide can be designated as the $E^i_{mn}$ mode, which has a predominant electric field component in the $i$ ($i = x$ or $y$) direction with $m-1$ and $n-1$ ($m, n \geqslant 1$) field zeros in the $x$ and $y$ directions, respectively. The refractive-index profile of the waveguide is characterized by two relative refractive-index steps, $\Delta_1$ and $\Delta_2$, defined by

$$\Delta_1 = \frac{n_1^2 - n_2^2}{2n_1^2} \tag{1}$$

and

$$\Delta_2 = \frac{n_1^2 - n_3^2}{2n_1^2}. \tag{2}$$

Manuscript received May 3, 1990; revised September 20, 1990.

The author is with the CSIRO Division of Applied Physics, Lindfield 2070, Australia.

IEEE Log Number 9041089.